

# Removal of Pb(II) Ion from the Wastewater Using Chitosan Coated Activated Carbon Derived from the Bark of Tamarindus Indica: Kinetic and Equilibrium Study

Hunge Sudhir\*

Department of Chemistry, Gondwana University, Gadchiroli (MS), India

\*Corresponding author: Hunge Sudhir, Department of Chemistry, Gondwana University, Gadchiroli (MS), India, Tel: +91 9960015562; E-mail: sudhir@chintamani.edu.in

**Received date:** September 26, 2022, Manuscript No. IPDCS-22-14637; **Editor assigned date:** September 28, 2022, PreQC No. IPDCS-22-14637 (PQ);

**Reviewed date:** October 12, 2022, QC No. IPDCS-22-14637; **Revised date:** October 17, 2022, Manuscript No. IPDCS-22-14637 (R); **Published date:** October 28, 2022, DOI: 10.36648/0976-8505.13.10.57

**Citation:** Hunge S (2022) Removal of Pb(II) ion from the Wastewater Using Chitosan Coated Activated Carbon Derived from the Bark of Tamarindus Indica: Kinetic and Equilibrium Study. Der Chem Sin Vol.13 No.10: 057.

## Abstract

Presence of heavy metals within the submarine systems has become a serious problem. Heavy metals are poisonous and non-biodegradable environmental pollutants that seriously threaten human health. The remediation of heavy metal-defiled water is an essential issue from each environmental and biological points of view. Thus there has been an honest deal of attention given to advance technologies for junking of heavy metal ions from contaminated water. Adsorption is one in every of the effective methods for removal of toxic heavy metal like Pb(II). In this study, the removal of Pb(II) from wastewater using chitosan based activated carbon deduced from the bark of Tamarindus indica was estimated. The prepared chitosan coated activated carbon was verified by Fourier Transform Infrared (FTIR) spectroscopy, X-Ray Diffraction (XRD), Thermogravimetric Analysis (TGA) and Scanning Electron Microscopy (SEM). The concentration of Pb<sup>2+</sup> ions were measured by flame-atomic absorption spectroscopy. Batch experiments were conducted to search out the influence of operating variables like pH effect, contact time, adsorbent dosage and initial concentration. The amount of Pb(II) adsorbed was found to vary with pH of the solution and maximum adsorption was found at a pH value of 6.0. The extent of Pb(II) uptake (mg/g) was found to increase with increase in initial concentration and contact time. Equilibrium was reached at 120 min. The experimental adsorption data were fitted to the Langmuir and Freundlich adsorption model and therefore the maximum adsorption capacity (qm) of CCTIAC was found to be 12.45 mg/g. Thus this disquisition verifies that the new advanced chitosan coated activated carbon prepared from the bark of Tamarindus indica as valuable material used as cost effective and less energy intensive adsorbent for the removal of Pb(II) from aqueous solution and wastewater waste with none chemical treatment, creating it user friendly bio-sorbent.

**Keywords:** Activated carbon; Adsorption; Bark of tamarindus indica; Lead; Chitosan

## Introduction

With the advance of civilization, human activities and progressive industrialization, the extend of heavy metals pollution is intensifying. This phenomenon is especially evident in surface water, soil water and shallow ground water. Water pollution is of particular because of the role played by water by water in ecosystem services [1]. Water may be valuable human resource but not permanent. Now a days, the source of water for living and natural waters in developing countries is now increasing polluted, especially heavy metals contamination [2-5]. Toxic heavy metals are one amongst the most contaminant of water resources [6]. Among the metals that are commonly released are copper, lead, zinc, silver, arsenic, antimony, iron selenium, chromium etc., [7]. Heavy metals and metalloids affects the standard of surface water and ground water resources mainly because they are non-biodegradable, toxic at low concentration and straightforward to accumulate within the tissue of assorted living organisms [8,9]. They will cause serious harm to human health from cancer to nervous system problems [10-12]. Lead is one amongst the foremost common and most toxic heavy metals found in industrial wastewater. It is released into the environment through mining, melting, galvanizing, and industrial metallurgical processes and from batteries, paints, ceramics, munitions, lead piping etc., [13,14]. This could have serious effects on the human nervous, reproductive, and circulatory systems, kidneys, and liver, with children the foremost vulnerable to intoxication [15,16]. The maximum contaminant level as per US Protection Agency (USEPA) is 0.006 mg/L, which is far more near to mercury [17]. Thus it's necessary to review and development of sustainable technology to get rid of these pollutants has gained attention in recent years. Various technologies are employed to get rid of heavy metals from contaminated water like chemical precipitation, ion exchange, adsorption, membrane filtration, reverse osmosis, solvent extraction, electro dialysis and electrochemical treatment, photo catalysis [18-22]. However these methods possess some drawback like inapplicability to large scale units together with expensive energy and chemical intensiveness. The adsorption process has gained growing research interest due to its easy operation and fleibility. Biosorption is an attractive method due

to large availability, low cost, operation facility and high heavy metal adsorption efficiency of the adsorbents [23-26]. An outside number of researchers have tried to use conventional and non-conventional adsorbents like carbonized biomass, uncarbonized powder biomass and activated carbon for removing lead from wastewater. Activated carbons prepared from agro-wastes are likely to possess properties cherish to those of commercially available activated carbon [27-32]. Actually, agro waste from crops and fruit production may be used as best suited material for preparation of low cost activated carbon. Most researchers have tried adsorption from aqueous solution utilizing different agricultural-based biosorbents, like tangerine peels, green marine macro algae, *Caulerpa scalpelliformis*; orange, pineapple and pomegranate peels; sunflower, potato, canola and walnut shell residues; almond shell; walnut shell; potato peel, lemon peel, orange peel, watermelon peel, tomato peel, coffee waste, apple peel, banana peel, decaf coffee waste, eggplant peel, carob peel and grape waste; orange peel [33-40]. Activated carbons prepared from apricot stone, coconut shell, groundnut husk, pecan nut shell, *Terminalia arjuna* nuts, etc., were successfully used for water and wastewater remediation by several researchers.

The present work reports the studies administered for the removal of lead from aqueous solution using activated carbon derived from bark of *Tamarindus indica* on which chitosan was coated. It's one among the most important families of seed plant belong to Fabaceae family and extensively employed in Ayurveda, Unani and Haemeopathic medicine and has becomes a cynosure of contemporary medicine [41]. Chitosan, {2-acetamido-2-deoxy- $\beta$ -D- glucose-(N acetylglucosamine)} a biopolymer, was chosen because it's excellent physicochemical properties. Hence, the impregnation of natural materials onto porous supports was conducted employing a synthetic polymeric host like chitosan. A polymeric sorbent like chitosan was used for water decontamination because it is an eco-friendly biopolymer that has attractive properties like biodegradability, biocompatibility, non-toxicity, is widely used and could be a low-cost adsorbent for metal-ion removal because of its high ratio of hydroxyl to amine groups [42,43]. The composite sorbent was characterized by FTIR and Scanning Electron Microscopy (SEM) studies. Batch isothermal equilibrium process was adopted at 308<sub>K</sub> to examine the efficiency of newly synthesized bio-sorbent for elimination of Pb<sup>+2</sup> from the aqueous solution. Experiments were allotted to check the effect of pH, adsorbent dosage, contact time and initial Pb<sup>+2</sup> concentration. The newly synthesized composite are proved to be excellent adsorbent which might be successfully used for removal of Pb<sup>+2</sup> from aqueous solution.

## Materials and Methods

### Chemicals

The chemicals used within the research had been of analytical grade. Chitosan, lead nitrate Pb(NO<sub>3</sub>)<sub>2</sub> (99%), potassium hydroxide pellets KOH (85%), and sodium hydroxide pellets NaOH (98%) were purchased from Merck (Mumbai, India). Hydrochloric acid HCl (~36%) and methanol (99.5%) have been

received from Global Marketing, Nagpur (India). All reagents have been used as obtained with none in addition treatment. Deionized water becomes used at some stage in the experimental process.

### Preparation of activated carbon from the bark of *Tamarindus Indica* (TIAC)

The bark of *Tamarindus indica* was gathered from the native place. The bark was cut into small portions and washed with tap water to put off the sand debris after which dealt with formaldehyde to keep away from launch its colouration into aqueous solution. Then, it was washed numerous instances with deionized water and solar dried for 5 days. After drying, the bark changed into subjected to pyrolysis technique for carbonization the usage of Muffle Furness at 800°C-900°C for 7-8 hrs in order that volatile constituents had been eliminated and residue was transferred right into a char. The char was then subjected to activation in microwave oven. The input electricity of microwave equipment was set at 360 W for 30 min. The ensuing activated carbon particles had been ground and sieved in 120-200  $\mu$ m size. This activated carbon was then washed with double distilled water and dried at 105°C for 24 hrs and kept in air tight bottle Figure 1.

### Preparation of Chitosan Gel

30 g of chitosan become delivered into 1000 ml of 10% oxalic acid with regular stirring. The mixture becomes warmed at 50°C-55°C for homogenous mixing. The chitosan-oxalic acid mixture becomes formed as a whitish viscous gel.

### Surface coating of TIAC with chitosan gel

500 ml of Chitosan gel turned into double diluted with distilled water and warmed to 45°C-50°C. 500 g of TIAC turned into slowly brought into diluted chitosan gel and shake using rotary shaker for 24 hr. The Chitosan Covered TIAC (CCTIAC) was then washed with deionized water and dried. The method was repeated 3-4 times to form thick coating of chitosan at the TIAC surface. The coated chitosan turned into 30 to 35% by weight. Oxalic acid was quantitatively neutralized through 0.5% sodium Hydroxide solution. The solid form of CCTIAC was filtered, washed with deionized water, dried and kept in air tight container (Figure 1).

### Characterization of CCTIAC

The structure of prepared composite became accomplished XRD. The morphology of the composite became tested with the aid of using SEM for functional groups assessment Fourier Transform Infrared (FTIR). The TGA analyses had been accomplished to screen the thermal stability of CCTIAC.

### Batch experiments of Pb(II) adsorption onto CCTIAC

The batch experiments were monitored using Flame Atomic Adsorption Spectrometry (AAS). Adsorption experiment was carried out by mixing a definite amount CCTIAC with 25 mL of Pb(II) solution in erlenmeyer flask. The pH of the mixture was

adjusted to the respective value of using 0.1 M HCL and 0.1 M NaOH. The mixture was shaken at 150 rpm at a definite temperature in a fixed time. The adsorbent-solution was filtered by using Whatman No.1 filter paper and the metal concentrations were analysed before and after adsorption using Atomic Absorption Spectrometer. The experiments were conducted to investigate effect of various parameters on Pb(II) adsorption onto CCTIAC namely, solution pH (2.0-9.0), contact time (10-180 min), initial Pb(II) concentration (10-100 mg/L) and adsorbent dosage (1 gm-10 gm).

### Theoretical calculations

500 ppm solution of  $Pb^{2+}$  was prepared by dissolving the appropriate quantity of  $Pb(NO_3)_2$  in deionized water. All operating solutions of the preferred concentrations have been obtained by dilution with deionized water. A calibrating curve was drawn using 5, 10, 15, 20, 25, 30, 35, 40, 45 and 50 ppm solutions. Sample concentrations have been calculated in keeping with the Beer-Lambert law with reference to the standard curve.

The equilibrium adsorption potential and the percentage elimination of  $Pb^{2+}$  ions ( $R_e\%$ ) have been calculated use of Equations (1) and (2),

$$q_t = \frac{(C_0 - C_t)V}{W} \dots 1$$

$$R_e = \left( \frac{C_0 - C_e}{W} \right) X 100 \dots 2$$

Where  $q_t$  (mg/g) is the adsorption capacity of CCTIAC for  $Pb^{2+}$  at time  $t$  (min) and  $C_0$  and  $C_e$  (mg/L) are the liquid phase concentrations of  $Pb^{2+}$  before and after adsorption, respectively.  $V$  (L) and  $W$  (g) are the volume of the adsorption solution and the weight of the dry adsorbent used, respectively.

### Adsorption isotherms

There are numerous adsorption isotherms to be had in literature, namely: Langmuir, Freundlich, BET, Temkin, Dubinin-Radushkevitch, Hill, Redlich-Peterson and Sips [44]. But on this study, we hired handiest two, Langmuir (equation 3) and Freundlich (equation 5) isotherms as they may be the maximum typically used theoretical adsorption isotherm models. These isotherms display the impact of initial concentration of metal ions and temperature at the adsorption process. We computed the adsorption capacities at equilibrium ( $q_e$ ) from Equation (4)

and (6) for Langmuir and Freundlich isotherms, respectively ° to acquire this, we used 100 mL beakers to prepare 50 mL volume of  $Pb^{2+}$  ion solutions of changing concentrations, as much as the maximum initial concentration of 200 mg/L. The pH of the solution was adjusted to the maximum value of pH 6.0 with usage of 0.1 M nitric acid and sodium hydroxide solutions. We proceeded to add 10 gm of the adsorbent and dispersed it with the aid of magnetic stirring at 600 rpm for a time of 4 h. After equilibrium changed into attained, the samples had been then filtered to be able to separate the cake adsorbent from the filtrate. We went directly to decide the residual  $Pb^{2+}$  ion concentrations with the aid of using AAS in the filtrate. We then used the result generate to best fit both models as given by Equation (4) & (6) in addition to the equilibrium relationship, Eq (7) [45].

Langmuir Isotherm equations

$$q_e = \frac{q_m b C_e}{1 + b C_e} \dots 3$$

$$\frac{C_e}{q_e} = \frac{1}{q_m b} + \frac{C_e}{q_m} \dots 4$$

Freundlich Isotherm equations

$$q_e = K_f C_e^{1/n} \dots 5$$

$$\ln q_e = \ln K_f + \frac{1}{n} C_e \dots 6$$

Equilibrium relationship equation

$$q_e = \frac{(C_0 - C_e)V}{W} \dots 7$$

In the equations(7),  $q_e$  represents the adsorbed metal ions per unit mass of adsorbent (mg/g);  $q_m$  represents the maximum adsorbed metal ions per unit mass of adsorbent (mg/g), and this is a characteristic Langmuir parameter;  $b$  represents the Langmuir adsorption equilibrium constant and is sometimes known as  $K_L$  the equilibrium constant (L/mg);  $K_f$  represents the adsorption capacity (L/mg);  $1/n$  represents the adsorption intensity (g/L) which is the relative distribution of the energy and the non-homogeneity of the adsorbate sites ( $n$  is adsorption energetics) Figure 1.



**Figure 1:** Bark of Tamarindus Indica, Chitosan Coated Activated Carbon (CCTIAC).

## Result and Discussion

### Characteristics of CCTIAC

**The XRD Pattern of CCTIAC:** Figure 2 suggests X-ray diffractograms of CCTIAC. XRD pattern of CCTIAC suggest two diffraction peaks at  $11^\circ$  and  $24^\circ$  which suggest the crystalline nature of the material. A peak at  $2\theta = 38^\circ$  to  $39^\circ$  once more proves the crystalline nature of the material. Pure chitosan additionally gives such function peak at  $2\theta = 29^\circ$  to  $30^\circ$  that determine the functional properties and crystallinity of chitosan [46]. The peak area for the peak at  $2\theta = 29^\circ$  to  $30^\circ$  within each the diffractogram is located to be very small.

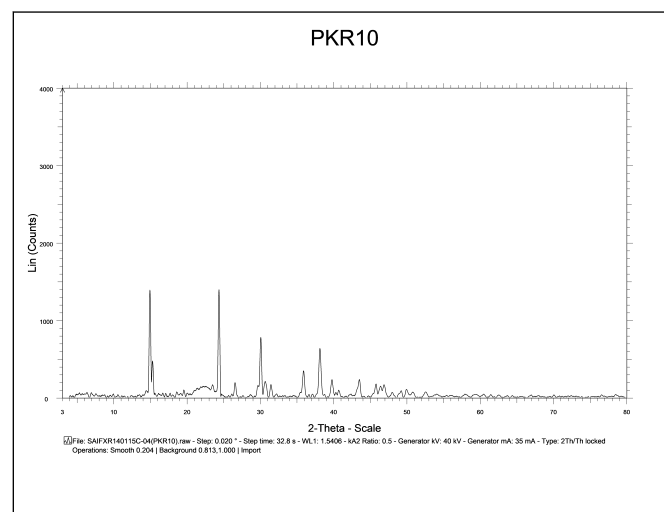


**Figure 2:** X-Ray Diffraction Pattern of Chitosan Coated Tamarindus Indica Activated Carbon (CCTIAC).

**FTIR Studies:** Figure 3 shows FTIR spectrum of CCTIAC. The looks of very broad band at  $3438.57\text{cm}^{-1}$  correspond to  $\text{-OH}$  stretching vibration of water and hydroxyl radical and  $\text{NH}$ -stretching vibration of free amino groups. The nature of broad band is due to the merging of bands of  $\text{-OH}$  and  $\text{-NH}$  group. FTIR of CCTIAC indicate the particular signal at  $1612.03\text{cm}^{-1}$  (strong absorption) and  $2284.47\text{cm}^{-1}$  (weak absorption), which can be assigned to the acylamino group and S-H vibration respectively. The peak at  $1314.26\text{cm}^{-1}$  corresponds to C-H and O-H deformation vibrations. Another band at  $1230\text{cm}^{-1}$  could be attributed to C-OH stretching. A band at  $779.13\text{cm}^{-1}$  represent  $\text{-CH}_2$  group rocking.

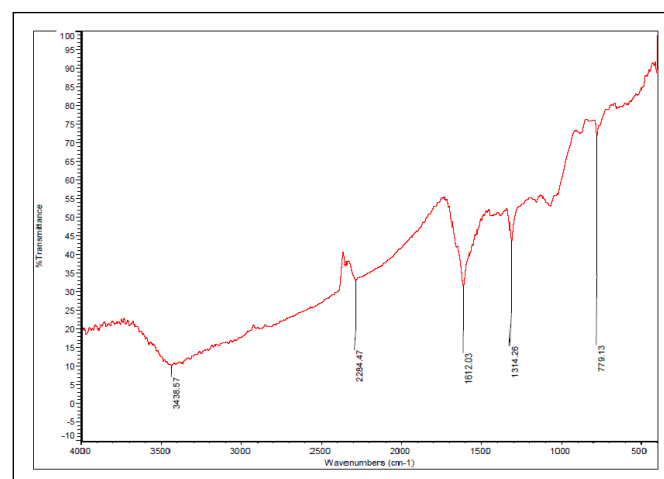


**Figure 3:** FTIR Spectrum of Chitosan Coated Tamarindus Indica Activated Carbon (CCTIAC).

SEM images of CCTIAC is given in Figure 4.

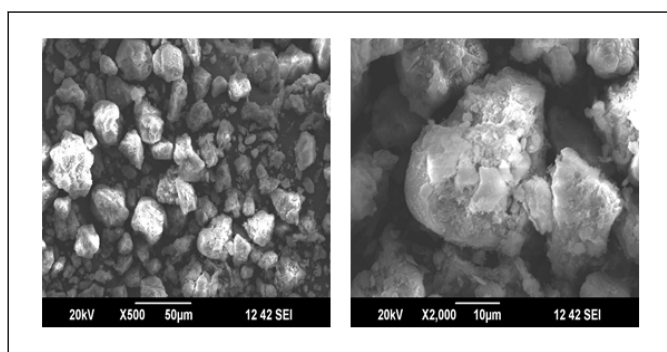


**Figure 4:** SEM image of Chitosan Coated Tamarindus Indica Activated Carbon (CCTIAC).

SEM images of CCTIAC show the porous and fibrous structure of CCTIAC adsorbent. The pores on the surface of CCTIAC are almost spherical and possess size within the range of 5-50  $\mu\text{m}$ . From SEM images, it's observed that the surface of CCTIAC is rough and folded which can be results of drying procedure. The external morphology of porous CCTIAC is appears to be stone like structured, which can be characterized by close packed array of columns.

T.G curve of CCTIAC is represented in Figure 5.

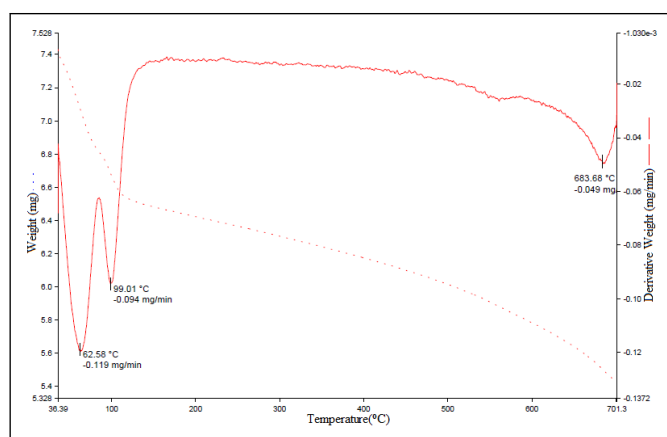


**Figure 5:** TG Curve of Chitosan Coated Tamarindus indica Activated Carbon (CCTIAC).

The first derivative peak is at very low temperature 62°C corresponding to the weight loss 5.50% of the material. This is may be the loss of water molecules loosely bounded on the surface of CCTIAC. The weight loss of 7.0% at 100°C represented the evaporation of moisture from the surface of the adsorbent. There is no weight loss between the temperature range of 100°C to 650°C shows the adsorbing material is thermally stable. But, at temperature 683.68°C, weight loss was found to be maximum *i.e.*, 25% which is degradation of chitosan composite and other organic molecules.

### Adsorbent dosage

Figure 6 shows the impact of adsorbent dose on the surface assimilation of CCTIAC for  $\text{Pb}^{2+}$  elimination. The proportion removal efficaciousness of  $\text{Pb}(\text{II})$  by CCTIAC considerably will increases with the rise in dose of CCTIAC over the vary 1-12 g/L and therefore the maximum removal efficiency of  $\text{Pb}(\text{II})$  ion *i.e.*,

92.7% occurred at the adsorbent dose of 12 g/L. It might be explained as increasing CCTIAC dose, the active sites offered for biosorption of  $\text{Pb}(\text{II})$  increased and consequently most removal of  $\text{Pb}(\text{II})$  take place. An extra increase of dose over 12 g/L didn't result in associated degree considerable increase of removal efficiencies. This result might be explained that the overlapping or aggregation of active sites at higher dose and decreasing in total sorbent surface area. Therefore, the maximum CCTIAC dose was 120 g/L.

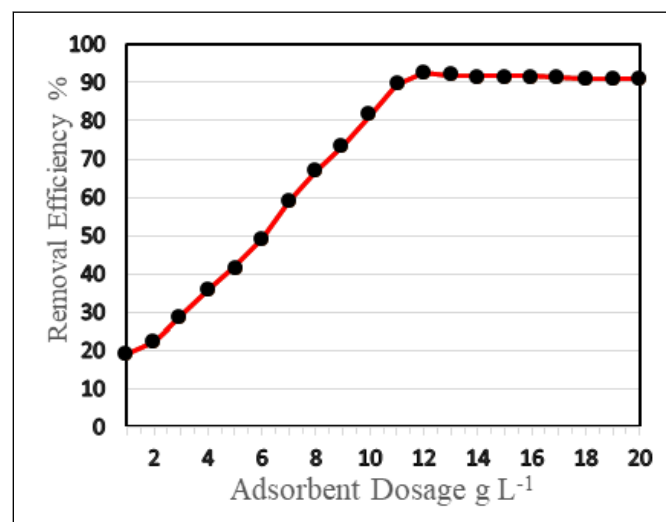


**Figure 6:** Effect of adsorbent dosage.

### pH effect

The adsorption of any significant heavy metals is considerably plagued by the pH of the solution, since it determines adsorbent properties like surface charge likewise because of the adsorbate evolution and degree of ionization in aqueous solutions. The result of pH of the solution on the  $\text{Pb}(\text{II})$  removal was observed with pH varying from 1 to 10 and are represented in Figure 7.

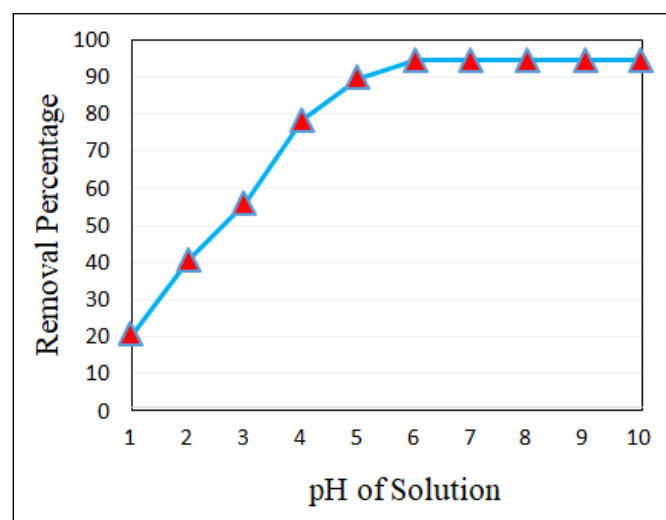


**Figure 7:** pH effect on  $\text{Pb}(\text{II})$  adsorption.

The  $\text{Pb}(\text{II})$  adsorption from aqueous solution could be kept about the pH value. It's ascertained that a gradual rise in the percentage of removal potency came about with a rise in pH from 1.0 to 6.0 and decreased slightly at the  $\text{pH} > 6.0$ . The

maximum percentage removal efficiencies of CCTIAC occurred at pH 6.0 and reached 94.6 %. It was well known that at lower pH, concentration of  $H^+$  in the solution is extremely high and therefore the functional groups in adsorbent surface were protonated. Hence,  $Pb(II)$  ion adsorption was hindered due to the competition between  $H^+$  and  $Pb^{2+}$  for the adsorption sites on the surface of the adsorbent. At higher pH ( $>pH_6$ ), the concentration of  $H^+$  in the solution low adsorption capability was decreased therefore the functional groups in adsorbent surface were deprotonated. Thus, additional  $Pb(II)$  ions were absorbable because of less competition between  $H^+$  and  $Pb^{2+}$ . Thus adsorption capability was decreased. This is often principally because of the formation of hydroxyl radical metal complexes when  $Pb(II)$  began to precipitate. The environment facilitates the formation of precipitate complex with metallic ions hooked up to the hydroxide ions forming  $Pb(OH)_2$  and negatively charged  $Pb(OH)_3$  complex ions. Furthermore at the  $pH > 7$ , lead hydroxide began to precipitate from the solution, creating the adsorption studies not possible.

### Effect of contact time on $Pb(II)$ removal

The Result of contact time on  $Pb(II)$  removal is allotted in figure 8.

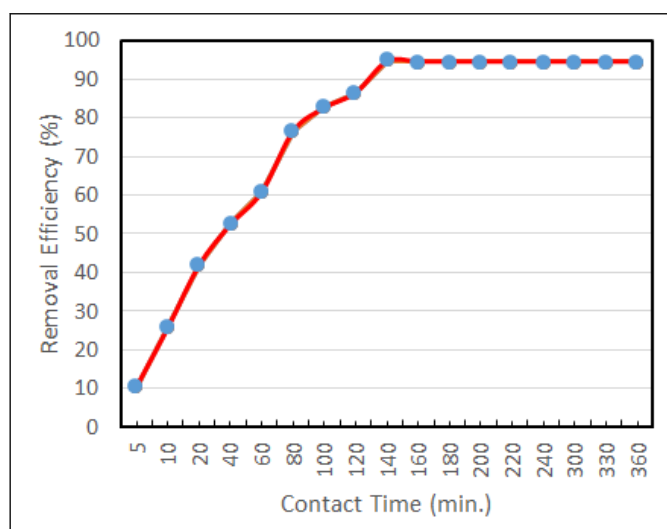


Figure 8: Effect of contact time.

It's indicated that, the  $Pb(II)$  removal efficiencies of CCTIAC increased quickly with increasing the contact time and reached the utmost and equilibrium set at 120 min. Initially biosorption of  $Pb(II)$  by CCTIAC was very fast and 75% of  $Pb(II)$  ions were adsorbed within 80 min. The equilibrium sorption was established after 140 min where the  $Pb(II)$  removal efficiencies increased up to 94.60% for CCTIAC. It showed no vital sweetening of removal potency with increasing contact time ( $>120$  min). Initially speedy uptake of  $Pb(II)$  ion due to the availability of unoccupied binding sites on the surface of adsorbent to interact with  $Pb(II)$  ion. As contact time extended, the sorption sites were majorly lined, decreasing the chance of  $Pb(II)$  ions to react with the functional groups on the adsorbent. Therefore equilibrium is reaching, the saturated binding sites

didn't facilitate the  $Pb(II)$  adsorption associate degree virtually constant adsorption capability.

### Effect of initial concentration

The initial metal ions concentrations  $Pb(II)$  in solution play a significant role as a good driving force in conquest mass transfer resistance of metal ions between the solution and adsorbent. As illustrated in Figure 9, that the percentage removal of  $Pb(II)$  attenuated from 93.88 to 69.4 for CCTIAC because the  $Pb(II)$  ion concentrations were raise from 5 to 285 mg/L . At lower  $Pb(II)$  concentration, most  $Pb(II)$  ions might bind on the adsorbent surface as there's an oversized magnitude relation of accessible surface assimilation site between  $Pb(II)$  present in the solution. As the initial  $Pb(II)$  concentration increased, the magnitude relation of unoccupied binding site is obtaining smaller whereas the lower removal of  $Pb(II)$  at high concentration could also be due to the dearth of accessible active sites on the surface of CCTIAC.

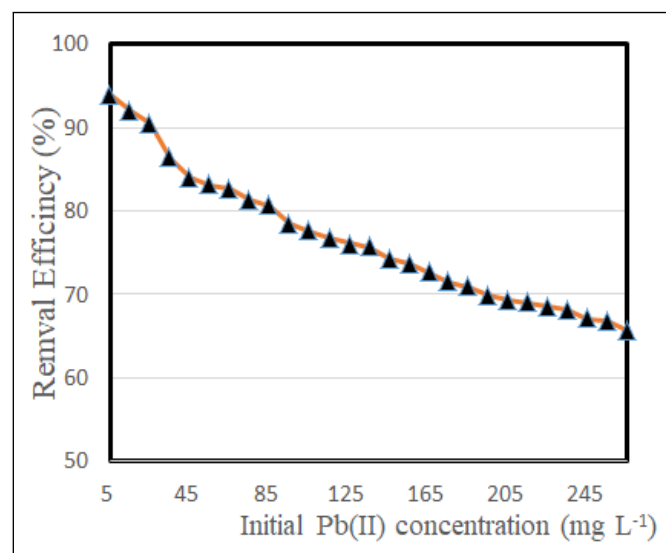


Figure 9: Effect of concentration on  $Pb(II)$  adsorption.

### Adsorption Isotherm

Langmuir and Freundlich isotherms are wont to explain the mechanism of adsorption and therefor the relationship between the number of adsorbed metal ion and also the concentration of metal ion remained in solution.

### Freundlich adsorption isotherm

The Freundlich model proposes an adsorption process that happens in multiple layers on a heterogeneous surface, and it also assumes that the adsorption capacity depends on the concentration of the sorbate in solution. The sorption capacity increases because the concentration increases. In the present study, the Freundlich equation is utilized for the adsorption of  $Cr(VI)$  on the adsorbents *i.e.*, CCTIAC and equilibrium data were well fitted in the linear plots of  $\log Q_e$  versus  $\log C_e$  as shown in Figure 10.

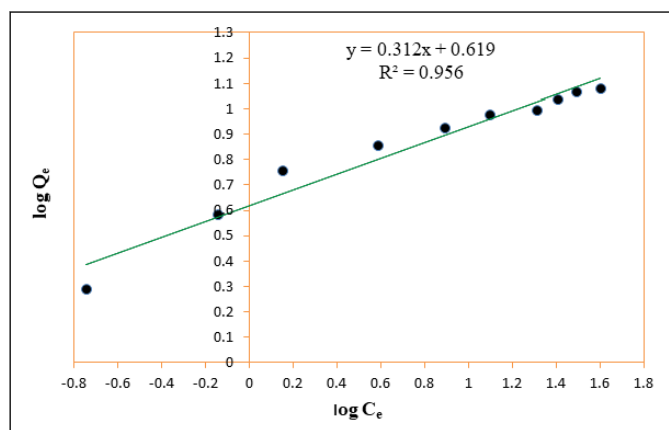


**Figure 10:** Freundlich Isotherm for the adsorption of Pb(II) on CCTIAC.

The values of adsorption capacity ' $k_F$ ' and intensity of adsorption ' $n$ ' were evaluated at 30°C for CCTIAC. The value of ' $k_F$ ' for CCTIAC was found to be 4.159 mg/ g. Quite higher values ' $k_F$ ' suggestive of accumulation number of adsorbate molecules (liquid phase) found in larger surface area of adsorbent (solid phase). The values of ' $n$ ' which provides idea about intensity of adsorption were found to be 3.12 for CCTIAC. The values of ' $n$ ' obtained are in good agreement of the adsorption favourable. The square of the coefficient of correlation ( $R^2$ ) values were found to 0.956 which means the most effective fitting of Freundlich isotherm for the adsorption system under investigation.

### Langmuir adsorption isotherm

Langmuir adsorption isotherm assumes that each one available adsorption active sites are similar, the adsorbable species doesn't interact, and a monolayer is created during adsorption. The linear style of the Langmuir isotherm was applied for calculation of the corresponding parameters, given in Table 1. The linear plots of versus for the adsorbents suggest the relevancy of the Langmuir isotherms represented diagrammatically in Figure 11.

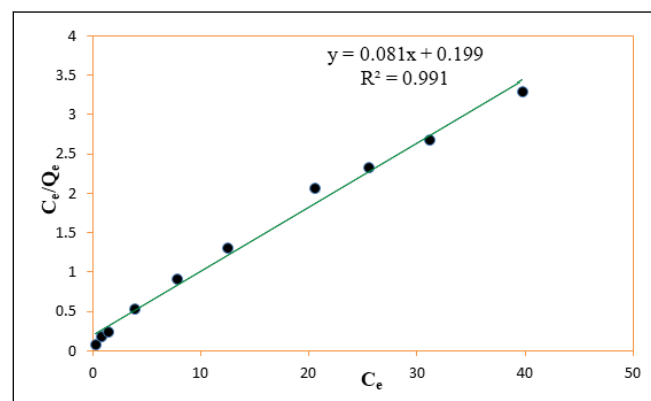


**Figure 11:** Langmuir Isotherm for the adsorption of Pb(II) on CCTIAC.

The values of ' $Q_m$ ' and ' $K_L$ ' were determined from slope and also the intercept of the plots. The coefficient of correlation ( $R^2$ ) values were found to be 0.991 which indicates the best fitting of Langmuir isotherm. The adsorption efficiency ' $Q_m$ ' value was found to be 12.346 mg/g for CCTIAC. The value of adsorption energy ' $K_L$ ' CCTIAC was found to be 0.4070. Hence, it are o ten conclude that the most adsorption corresponds to a saturated monolayer of adsorbate molecules on the adsorbent surface. The constant adsorption energy values suggest that there is no transmission of the adsorbate in the plane of absorbent surface. The favorability of the adsorption process, the separation factor ' $R_L$ ' values were calculated and was found in between 0-1 which suggest confirmation regarding favourable adsorption process.

It was concluded that the two models were reasonably suitable for describing adsorption. However, the Freundlich equation provided an improved it than the Langmuir equation. The value of  $K_F$  indicated moderate affinity for  $Pb^{2+}$ . Freundlich model is additionally characterized by the heterogeneity factor  $1/n$  i.e.,  $0.1 < 1/n < 1.0$  indicates good adsorption of Pb(II) ions onto CCTIAC . From the isotherm data in Table 1, it implies that the Freundlich model well it the adsorption, suggesting a chemical adsorption process, as indicated by the  $n$  value 3.115, the heterogeneity factor.

Adsorbent	Freundlich				Langmuir			
	$n$	$1/n$	$K_F$ (mg/g)	$R^2$	$Q_m$ (mg/g)	$K_L$	$R^2$	$R_L$
CCTIAC	3.115	0.321	4.159	0.956	12.45	0.407	0.991	0.197

**Table 1:** Langmuir and Freundlich isotherm parameters for  $Pb^{2+}$  adsorption on CCTIAC.

### Conclusion

- The study indicates that the activated carbon successfully prepared from the bark of Tamarindus indica.
- The Surface coating of recently prepared activated carbon with Chitosan was successfully done and will act as an effective and potentially low-cost adsorbent for lead removal from aqueous solution.

- The CCTIAC were with success characterized by X-ray diffraction, Fourier-transform infrared, scanning electron microscopy and thermal analysis.
- Batch studies were carried out under different conditions like dose of adsorbent, pH of solution, initial Pb(II) concentration and contact time to judge the adsorption potency of Pb(II) ions on CCTIAC.
- The adsorption of Pb(II) on CCTIAC was found to be pH-dependent. The best removal potency 93.66% was obtained at pH 6. The initial concentration of the Pb(II) ion in solution was found to possess a pronounced result on the adsorption method.

- Kinetic experiments proved that the removal potency of Pb(II) ion from aqueous solutions was speedy and equilibrium was achieved at intervals 140 min.
- The adsorption equilibrium of Pb was satisfactorily described by both the Langmuir and Freundlich equations along the studied concentration range, with better correlation to the Freundlich isotherm. The most adsorption (qm) calculated from the Langmuir equation was 12.45 mg/ g.

## Acknowledgement

The author is highly thankful to Dr. P.K. Rahangdale, Bhawabhuti Mahavidyalaya, Amgaon and Prof. Mamata Lanjewar, PGTD Chemistry; RTM Nagpur University Nagpur, for their valued guidance, moral provision, timely help and persistent encouragement during the course of this investigation. The authors also thanked Scientist In-charge, SAIF, STIC, Cochin University, Cochin for FTIR and SEM analysis of the sample. The authors are also thankful to the Managing Director of Deenee Chemical Laboratory (DCL), Chandrapur, for letting us accessing the atomic absorption spectrophotometer and UV-Visible spectrophotometer.

## References

- Liu S, Lei Y, Zhao J (2021) Research on ecosystem services of water conservation and soil retention: A bibliometric analysis. *Env Sci Pollu Res* 28: 2995-3007.
- Minh TD, Lee BK (2018) Ternary cross coupled nanohybrid for high efficiency 1H-benzo[d]imidazole, Chemisorption. *Env Sci & Pollution Res* 25(22): 21901-21914.
- Minh TD, Lee BK, Linh PH (2018) Highly efficient removal of emerging organic compound 1,3 benzodiazole using novel triangular coordination of magnetic polymer nanohybrid [C<sub>2</sub>H<sub>5</sub>OH]-MNP s@Y-APTEs@GO. *Research on Chemical Intermediates* 44(11): 6515-6536.
- Minh TD, Lee BK, Nguyen MT (2018) Methanol dispersed of ternary Fe<sub>3</sub>O<sub>4</sub>@Y-APS/GO based nanohybrid for novel removal of benzotriazole from aqueous solution. *J of Management* 209: 452-462.
- Minh TD, Lee BK (2017) Effect of functionality and textural characteristics on the removal of Cd(II) by ammoniated and chlorinated nanoporous activated carbon. *Journal of Material Cycles and Waste Management* 19(3): 1022-1037.
- Yang J, Hour B, Wang J, Tian B, Bi J, et al. (2019) Nanomaterials for the removal of heavy metals from waste water. *Nanomaterials* 9: 424.
- Akcil A, Koldas S (2006) Acid Mine Drainage (AMD): Causes, treatment and case studies. *J Clean Prod* 14: 1139-1145.
- Carolyn CF, Kumar PS, Saravanan A, Joshiba GJ, Naushad M (2017) Efficient technique for removal of toxic heavy metals from aquatic environment: A review. *J Enviro Che Eng* 5: 2782-2799.
- Vardhan KH, Kumar PC, Panda RC (2019) A review on heavy metals pollution, toxicity and remedial measures: Current trends and future Perspective. *J Mol Liq* 290: 111-197.
- Visa M (2016) Synthesis and characterization of new zeolite materials obtained from fly ash for heavy metals removal in advanced waste water treatment. *Powder Technol* 294: 338-347.
- Malik A (2004) Metal bioremediation through growing cell. *Environ Int* 30: 261-278.
- Ziagova M, Dimitriadis G, Aslanidou D, Papaioannou X, Litopoulo U, et al. (2007) Comparative study of Cd(II) and Cr(VI) biosorption on staphylococcus xylosus and Pseudomonas sp. Single and binary mixture. *Bioresour Technol* 98: 2859-2865.
- Wongrod S, Simon S, Guibaud G, Lens PNL, Pechaud Y, et al. (2018) Lead sorption by biochar produced from digestates: Consequences of chemical modification and washing. *J Environ Manag* 219: 277-284.
- Seema KM, Mamba BB, Njuguna J, Bakhtizin RZ, Mishra AK (2018) Removal of lead (II) from aqueous waste using (CD-PCL-TiO<sub>2</sub>) bio-nanocomposites. *Int J Biol Macromol* 109: 136-142.
- Beltrame KK, Cazetta AL, de-Souza PSC, Spessato L, Silva TL, et al. (2018) Adsorption of caffeine on mesoporous activated carbon fibers prepared from pineapple plant leaves. *Ecotoxicol Environ Saf* 147: 64-71.
- Sone H, Fugetsu B, Tanaka S (2009) Selective elimination of lead(II) ions by alginate/polyurethane composite foams. *J Hazard Mater* 162: 423-429.
- Tanveer MAS (2020) Adsorption of Pb(II) from wastewater by natural and synthetic adsorbents. *Biointerface Research in Applied Chemistry* 10(5): 6522-6539.
- Byambaa M, Dolgor E, Shimori K, Suzuki Y (2018) Removal and recovery of heavy metals from industrial wastewater by precipitation and foam separation using lime and casein. *Journal of Environmental Science and Technology* 11: 1-9.
- Haleem D (2020) Aerobic and anaerobic removal of lead and mercury via calcium carbonate precipitation mediated by statistically optimized nitrate reductases. *Scientific Report* 10: 4029.
- Lai YC, Chang YR, Chen ML, Lo YK, Lai JY, et al. (2016) Poly(vinyl alcohol) and alginate crosslinked matrix with immobilized Prussian blue and ion exchange resin for cesium removal from waters. *Bioresource Technology* 214: 192-198.
- Lalmi A, Bouhidel KA, Sahaoui B, Anfif CH (2018) Removal of lead from polluted waters using ion exchange resin with Ca(NO<sub>3</sub>)<sub>2</sub> for elution. *Hydrometallurgy* 178: 287-293.
- Novais RM, Buruberry LH, Seabra MP, Labrincha JA (2016) Novel porous fly-ash containing geopolymer monoliths for lead adsorption from wastewaters. *J Hazard Mater* 318: 631-640.
- Alghamdi AA, Al-Odayni AB, Saeed WS, Al-Kahtani A, Alharthi FA, et al. (2020) Efficient adsorption of lead(II) from aqueous phase solutions using polypyrrole-based activated carbon. *Materials* 12.
- Landaburu-Aguirre J, Pongracz E, Peramaki P, Keiski RL (2010) Micellar-enhanced ultrafiltration for the removal of cadmium and zinc: Use of response surface methodology to improve understanding of process performance and optimization. *J Hazard Mater* 180: 524-534.
- Rahmanian B, Pakizeh M, Esfandyari M, Heshmatnezhad F, Maskooki A (2011) Fuzzy modeling and simulation for lead removal using micellar-enhanced ultrafiltration (MEUF). *J Hazard Mater* 192: 585-592.
- Petricic I, Korenak J, Povodnik D, Helix-Nielsen C (2015) A feasibility study of ultrafiltration/reverse osmosis (UF/RO)-based wastewater treatment and reuse in the metal finishing industry. *Journal of Clean Production* 101: 292-300.

27. Yoon J, Amy G, Chung J, Sohn J, Yoon Y (2009) Removal of toxic ions (chromate, arsenate, and perchlorate) using reverse osmosis, nanofiltration, and ultrafiltration membranes. *Chemosphere* 77: 228-235.
28. Lertlapwasin R, Bhawawet N, Imyim A, Fuangswasdi S (2010) Ionic liquid extraction of heavy metal ions by 2-aminothiophenol in 1-butyl-3-methylimidazolium hexafluorophosphate and their association constants. *Sep Purif Technol* 72: 70-76.
29. Ferniza-García F, Amaya-Chávez A, Roa-Morales G, Barrera-Díaz CE (2017) Removal of pb, cu, cd, and zn present in aqueous solution using coupled electrocoagulation-phytoremediation treatment. *International Journal of Electrochemistry*.
30. Zhang J, Li Y, Xie X, Zhu W, Meng X (2018) Fate of adsorbed Pb(II) on graphene oxide under variable redox potential controlled by electrochemical method. *J Haz Mat* 367: 152-159.
31. Mimouni I, Bouzuani A, Naciri Y, Boujnah M, El-Beghiti MA, et al. (2021) Effect of heat treatment on photocatalytic activity of  $\alpha$ -Fe<sub>2</sub>O<sub>3</sub> nanoparticles toward diclofenac elimination. *Envi Sci Poll Res* 29: 7984-7996.
32. Naciri Y, Hsini A, Bouziani A, Djellabi R, Ajaml Z, et al. (2021) Photocatalytic oxidation of pollutants in gas phase via Ag<sub>3</sub>PO<sub>3</sub>-based semiconductor catalyst: Recent progress, new trends and future perspective. *Crit Rev Environ Sci Technol* 1-44.
33. Abdic S, Memic M, Sabanovic E, Sulejmanovic J, Begic S (2018) Adsorptive removal of eight heavy metals from aqueous solution by unmodified and modified agricultural waste: tangerine peel. *Int J Environ Sci Technol* 15: 2511-2518.
34. Jayakumar V, Govindaradjane S, Rajasimman M (2021) Efficient adsorptive removal of zinc by green marine macro alga caulerpa scalpelliformis-characterization, optimization, modelling, isotherm, kinetic, thermodynamic, desorption and regeneration studies. *Surf Interfaces* 22: 100798.
35. Turkmen KSN, Kipcak AS, Derun EM, Tugrul N (2020) Removal of zinc from wastewater using orange, pineapple and pomegranate peels. *Int J Environ Sci Technol*.
36. Feizi M, Jalali M (2015) Removal of heavy metals from aqueous solutions using sunflower, potato, canola and walnut shell residues. *J Taiwan Inst Chem Eng* 54: 125-136.
37. Coruh S, Geyikli F, Kilic E, Coruh U (2014) The use of NARX neural network for modelling of adsorption of zinc ions using activated almond shell as a potential bio sorbent. *Bioresour Technol* 151: 406-410.
38. Segovia-Sandoval SJ, Ocampo-Pérez R, Berber-Mendoza MS, Leyva-Ramos R, Jacobo-Azuara A, Medellín-Castillo NA (2018) Walnut shell treated with citric acid and its application as biosorbent in the removal of Zinc(II). *J Water Process Eng* 25: 45-53.
39. Massimi L, Giuliano A, Astolfi ML, Congedo R, Masotti A, et al. (2018) Efficiency evaluation of food waste materials for the removal of metals and metalloids from complex multi-element solutions. *Materials* 11(3): 334.
40. Santos CM, Dweck J, Viotto RS, Rosa AH, Morais LC (2015) Application of orange peel waste in the production of solid biofuels and biosorbents. *Bioresour Technol* 196: 469-479.
41. Kumar CS, Bhattacharya S (2008) Tamarind seed: Properties, processing and utilization. *Critical Reviews in Food Science and Nutrition* 48: 1-20.
42. Mashile GP, Mpupa A, Nqombolo A, Dimpe KM, Nomngongo PN (2020) Recyclable magnetic waste tyre activated carbonchitosan composite as an effective adsorbent rapid and simultaneous removal of methylparaben and propylparaben from aqueous solution and wastewater. *J Water Process Eng* 33: 101011.
43. Zhang Y, Xue Q, Li F, Dai J (2019) Removal of heavy metal ions from wastewater by capacitive deionization using polypyrrole/chitosan composite electrode. *Adsorpt Sci Technol* 37(3-4): 205-216.
44. Kegl T, Kosak A, Obnik A, Novak Z, Kovac-Kralj A, Ban I (2020) Adsorption of rare earth metals from wastewater by nanomaterials: A review. *J Hazard Mater* 386: 1211632.
45. El-Aila HJ, Elsousy KM, Hartany KA (2016) Kinetics, equilibrium and isotherms of the adsorption of cyanide by MDFSD. *Arab J Chem* 9: S198-S203.
46. Trang ST, Wah WT, Nguyen TQ, Chuen HN, Wellem FS (2006) Functional characteristics of shrimp chitosan and its membranes as affected by the degree of deacetylation. *Bioresources Technology* 97: 659-663.